

# Severe-Thunderstorm Reanalysis Environments and Collocated Radiosonde Observations

VICTOR A. GENSINI

*College of DuPage, Glen Ellyn, Illinois*

THOMAS L. MOTE

*University of Georgia, Athens, Georgia*

HAROLD E. BROOKS

*National Severe Storms Laboratory, Norman, Oklahoma*

(Manuscript received 15 August 2013, in final form 1 November 2013)

## ABSTRACT

This research compares reanalysis-derived proxy soundings from the North American Regional Reanalysis (NARR) with collocated observed radiosonde data across the central and eastern United States during the period 2000–11: 23 important parameters used for forecasting severe convection are examined. Kinematic variables such as 0–6-km bulk wind shear are best represented by this reanalysis, whereas thermodynamic variables such as convective available potential energy exhibit regional biases and are generally overestimated by the reanalysis. For thermodynamic parameters, parcel-ascent choice is an important consideration because of large differences in reanalysis low-level moisture fields versus observed ones. Results herein provide researchers with potential strengths and limitations of using NARR data for the purposes of depicting climatological information for hazardous convective weather and initializing model simulations. Similar studies should be considered for other reanalysis datasets.

## 1. Introduction

Past research using reanalysis data has provided significant insight into the understanding of climatological distributions and trends of parameters associated with severe convective storms (e.g., Brooks et al. 2003, 2007; Craven et al. 2004; Gensini and Ashley 2011; Allen and Karoly 2014). In essence a three-dimensional best-guess snapshot of the atmosphere in time, reanalysis aims to provide an objectively modeled baseline dataset that serves to fill data-void areas in the coarse-density radiosonde network. The goal of reanalysis is to assimilate data from multiple observation platforms (e.g., surface observations, satellite information, and radiosondes) into a numerical weather prediction model to provide a climatological snapshot of conditions that is as close to

reality as possible. The final product of atmospheric reanalysis is a large (potentially global) dataset that has greater spatiotemporal resolution than that of observed sounding data. These data are regularly used to conduct historical meteorological analyses, create climatological information and graphics, or initialize boundary conditions for historical model simulations.

Reanalysis datasets are currently a popular data source for researchers (we counted 3140 peer-reviewed journal articles from 2010 to 2011 with “reanalysis” in the title or abstract), but little peer-reviewed research has examined how the filtered nature (e.g., limited vertical levels) of reanalysis data may affect convectively pertinent variables. For example, a documented problem of reanalysis for convective purposes is the overestimation of environments that are favorable for hazardous convective weather (HCW) in southern Texas (Gensini and Ashley 2011). Thus, it is hypothesized that the limited vertical resolution from the reanalysis model surface to ~3000 m AGL poorly captures sharp changes in temperature, affecting the calculation of convective inhibition (CIN) produced

---

*Corresponding author address:* Vittorio A. Gensini, Dept. of Meteorology, College of DuPage, 425 Fawell Blvd., Glen Ellyn, IL 60137.  
E-mail: gensiniv@cod.edu

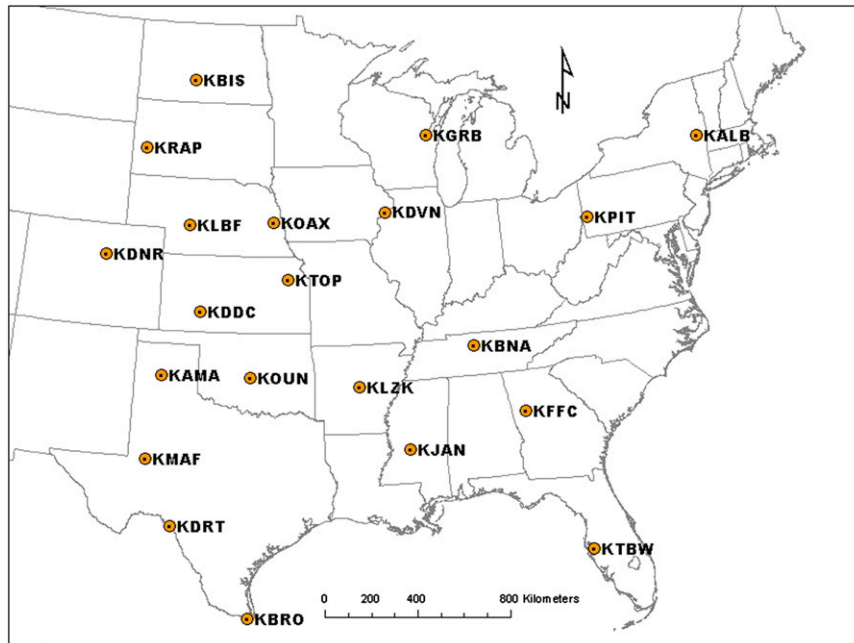


FIG. 1. Locations of 21 radiosonde stations used in this study.

by an elevated mixed layer (EML), as described by Lanicci and Warner (1991). A recent international study revealed similar problems with CIN calculations over HCW-favored regions of Australia (Allen and Karoly 2014). Thus, the purpose of this research is to examine the modeled reanalysis proxy soundings in conjunction with collocated observed sounding data, specifically analyzing key convective variables. Results from this study provide researchers with potential strengths and limitations of using North American Regional Reanalysis (NARR) data for purposes of depicting HCW climatological information and initializing model simulations.

## 2. Background

Two other studies have examined the relationship between radiosonde data and reanalysis output for purposes of studying severe convection (Lee 2002; Allen and Karoly 2014). Lee (2002) showed that reanalysis proxy soundings provide a reasonable approximation of the convective environment when compared with collocated soundings: kinematic variables were found to be best represented by reanalysis whereas thermodynamic parameters sometimes contained large differences that resulted from errors in low-level moisture fields (Lee 2002). Lee's (2002) research was conducted with coarse-resolution global reanalysis data, whereas this study uses a higher-spatial resolution reanalysis, both in the vertical and horizontal planes, in an attempt to best compare the observed and reanalyzed convective environment.

Allen and Karoly (2014) examined European Centre for Medium-Range Weather Forecasts Interim Re-Analysis (ERA-Interim) data in comparison with observations for ~20 radiosonde stations and ~3700 soundings over Australia. Results from Allen and Karoly (2014) support the findings shown in Lee (2002).

### *a. Reanalysis datasets for convective research*

Coarse-resolution global reanalysis datasets such as the National Centers for Environmental Prediction–National Center for Atmospheric Research (NCEP–NCAR) global reanalysis (Kalnay et al. 1996) have been utilized (Brooks et al. 2003, 2007) for global perspectives of severe convective environments over long time periods (available from 1949 to the present). A higher-spatiotemporal-resolution reanalysis over North America (NARR; Mesinger et al. 2006) was used by Gensini and Ashley (2011) to examine severe convective environments over the United States in greater detail (available from 1979 to the present). NARR provides researchers with a temporally consistent climate-data suite for North America (Mesinger et al. 2006) and is preferred over other global reanalysis data for this study because of its superior vertical resolution. Native NARR gridded binary data have a horizontal resolution of 32 km, a vertical resolution of 45  $\sigma$  layers, and temporal resolution of 3 h. NARR uses the 2003 operational Eta Model as part of the assimilation cycle (G. Manikin 2010, personal communication). In comparison, the NCEP–NCAR global reanalysis has a 210-km horizontal resolution, vertical

resolution of 28  $\sigma$  layers, and temporal resolution of 6 h. Using NARR data for this study provides superior vertical resolution, but the corresponding horizontal domain is limited to North America.

### 3. Method

Raw radiosonde data for 0000 UTC from 2000 to 2011 were obtained from the University of Wyoming's online data archive (<http://weather.uwyo.edu/upperair/sounding.html>) for 21 stations east of the U.S. continental divide (Fig. 1), where HCW is climatologically favored (Brooks et al. 2003; Gensini and Ashley 2011). Synoptic off-hour (i.e., 1800, 2100 UTC, etc.) radiosonde launches were omitted from this study because of their limited sample size. Reanalysis proxy soundings were obtained by extracting point data from 0000 UTC NARR files using the Model Gridded Binary (GRIB) Data Sounding program (GRBSND), available in the Weather Processor 6 (WXP) software package from Unisys. Customized Python software routines were used to calculate 23 different convectively important variables and composite parameters (listed with their abbreviations in Table 1), to quality control sounding data, and to store values in comma-separated-value (CSV) format. In an effort to evaluate only surface-based convectively favorable environments, only soundings with nonzero surface-based CAPE were considered for this study.

As previously mentioned, low-level thermodynamic errors could be particularly problematic for variables that rely on vertical integration (e.g., CAPE, or any composite parameter that utilizes CAPE in its calculation). This study employs different parcel-ascent methods on all thermodynamic parameters to see whether a "best choice" exists for researchers using NARR. Thus, two parcel-ascent trajectories were calculated [100-hPa mixed layer (ML) and surface-based (SB)] and were applied to all thermodynamic parameters and composite indices. A 100-hPa ML parcel averages the thermodynamic values (i.e., temperature  $T$  and dewpoint  $T_d$ ) in the lowest 100 hPa of the atmosphere, whereas an SB parcel uses the  $T$  and  $T_d$  at the surface of the atmosphere (or model) to calculate various indices. The distributed NARR dataset has five vertical levels that fall in the lowest 100 hPa of the model (1000, 975, 950, 925, and 900 hPa), whereas a typical radiosonde launch will have approximately eight data points in the lowest 100 hPa. Note that all parcel routines in this study utilize the virtual temperature correction, because it can result in larger and more realistic values of CAPE (Doswell and Rasmussen 1994).

Values of the square of correlation coefficient  $R^2$  and root-mean-square error (RMSE) (along with standard linear regression slope and  $y$ -intercept values) were

TABLE 1. Convective variables and composite indices examined in this study.

Abbreviation	Parameter
SBCAPE	Surface-based convective available potential energy
MLCAPE	100-hPa mixed-layer convective available potential energy
SBCIN	Surface-based convective inhibition
MLCIN	100-hPa mixed-layer convective inhibition
SBLI	Surface-based lifted index (calculated at 500 hPa)
MLLI	100-hPa mixed-layer lifted index (calculated at 500 hPa)
SBLCL	Surface-based lifting condensation level
MLLCL	100-hPa mixed-layer lifting condensation level
03SRH	0–3-km storm relative helicity
01SRH	0–1-km storm relative helicity
7/5LR	700–500-hPa lapse rate
SCP	Supercell composite parameter (using a surface-based parcel)
STP	Significant tornado parameter (using a surface-based parcel)
01EHI	0–1-km energy helicity index (using a surface-based parcel)
FRZGLVL	Freezing level
SFCT <sub>d</sub>	Surface dewpoint
850T <sub>d</sub>	850-hPa dewpoint
200WND	200-hPa wind velocity
500WND	500-hPa wind velocity
850WND	850-hPa wind velocity
T <sub>c</sub>	Convective temperature
6BWD	0–6-km bulk wind difference
CB	Craven–Brooks significant severe parameter (using a surface-based parcel)

computed between grouped observed sounding-derived parameter values and the concurrent pair of reanalysis values. RMSE was calculated with the formula [following the method of Wilks (1995)]

$$\text{RMSE} = \left[ \frac{1}{N} \sum (\text{NARR}_n - \text{OB}_n)^2 \right]^{1/2},$$

where the sum is from  $n = 1$  to  $N$ ,  $N$  is the number of values in each group,  $\text{NARR}_n$  is the  $n$ th reanalysis value, and  $\text{OB}_n$  is the  $n$ th observed value. Thus, RMSE represents a typical error (reanalysis minus observed) magnitude for each group of paired observations. To visualize the results, 2D histograms were plotted for all stations (Fig. 1) and all variables (Table 1). All 2D histograms were constructed using Python and the Matplotlib extension library software (Hunter 2007). The 1:1 black line on each plot represents a perfect correlation (i.e., NARR value = observed radiosonde value).

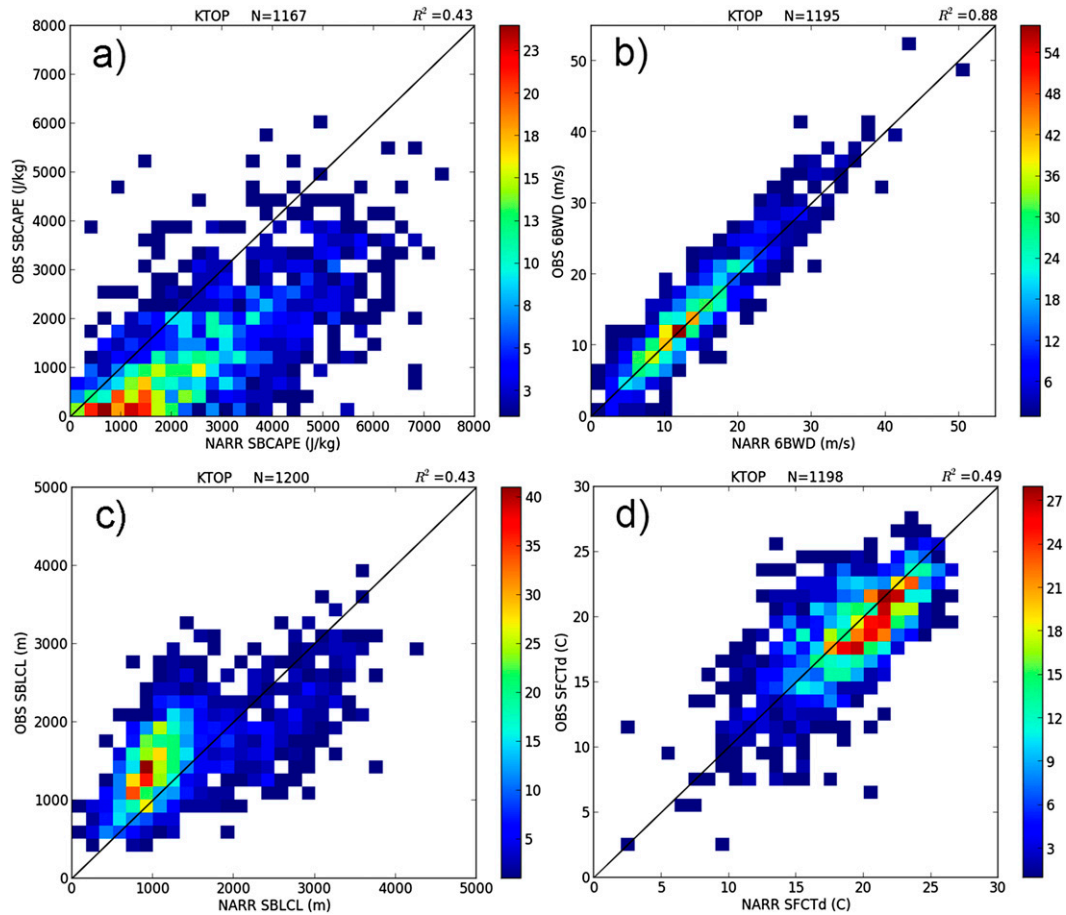


FIG. 2. Comparison between NARR and observed (a) SBCAPE, (b) 6BWD, (c) LCL, and (d)  $SFCT_d$  for all events during 2000–11 with nonzero SBCAPE at KTOP.

#### 4. Results

The 2D histograms were useful in comparing the distributions between NARR and observed soundings (Fig. 2). For example, in Fig. 2a, one can see that SBCAPE values at Topeka, Kansas (KTOP), have a positive bias (i.e., NARR SBCAPE tends to exceed observed SBCAPE values) with an RMSE value of  $1637 \text{ J kg}^{-1}$ . In Fig. 2b, however, good correlation ( $R^2 = 0.88$ ) is found between NARR and observed 6BWD, exhibiting an RMSE of only  $2.7 \text{ kt}$  ( $1 \text{ kt} \approx 0.51 \text{ m s}^{-1}$ ).

##### a. Correlation

Table 2 displays  $R^2$  values for all 23 parameters and 21 sounding locations. In broad terms,  $R^2$  values are found to be higher for kinematic variables for variables such as 6BWD and show less correlation for thermodynamic variables such as SBCAPE. This is an expected result, because  $R^2$  values are typically lower for derived variables and composite parameters, where compounding

error (e.g., calculation of a product) reduces correlation values. In addition, composite parameters such as STP may be biased with errors from other variables that enter the calculation (e.g., 01SRH). Out of the 23 parameters examined, FRZGLVL exhibited the highest  $R^2$  values and STP exhibited the lowest values regardless of station location. Seven variables (7/5LR, FRZGL, 850WND, 500WND, 200WND, 6BWD, and CB) exhibited good ( $\geq 0.75$ ) correlation, nine variables (SBCAPE, SBLI, SBLCL, 03SRH, 01SRH, SCP, 01EHI,  $SFCT_d$ , and  $T_c$ ) displayed fair ( $0.25 > x > 0.75$ ) correlation, and seven variables (MLCAPE, SBCIN, MLCIN, MLLI, MLLCL, STP, and  $850T_d$ ) presented poor ( $\leq 0.25$ )  $R^2$  values (Table 3).

Perhaps most interesting are the relatively low  $R^2$  values associated with  $SFCT_d$  and  $850T_d$ , because these values are not derived.  $SFCT_d$   $R^2$  values ranged from 0.37 to 0.63, and  $850T_d$   $R^2$  values ranged from 0 to 0.43, which would be associated with fair to poor agreement (respectively) in this context. This is important, because

TABLE 2. The  $R^2$  values for all parameters and stations analyzed in this study.

	KTOP	KTBW	KRAP	KPIT	KOUN	KOAX	KMAF	KLZK	KLBF	KJAN	KGRB	KFFC	KDVN	KDRT	KDNR	KDDC	KBRO	KBNA	KBIS	KAMA	KALB	Avg
SBCAPE	0.43	0.17	0.35	0.24	0.41	0.38	0.13	0.31	0.39	0.21	0.40	0.19	0.37	0.32	0.19	0.37	0.33	0.32	0.50	0.33	0.25	0.31
MCAPE	0.19	0.00	0.01	0.15	0.01	0.22	0.00	0.05	0.05	0.00	0.37	0.01	0.33	0.20	0.00	0.05	0.20	0.14	0.22	0.00	0.26	0.12
SBCIN	0.12	0.12	0.07	0.12	0.20	0.18	0.04	0.05	0.12	0.20	0.16	0.14	0.08	0.22	0.00	0.21	0.40	0.05	0.10	0.06	0.06	0.13
MFCIN	0.21	0.01	0.11	0.07	0.02	0.09	0.03	0.11	0.13	0.04	0.22	0.00	0.07	0.20	0.00	0.13	0.38	0.07	0.16	0.10	0.19	0.11
SBLI	0.46	0.27	0.23	0.22	0.46	0.48	0.16	0.35	0.37	0.25	0.39	0.24	0.37	0.30	0.14	0.37	0.36	0.31	0.44	0.30	0.23	0.32
MLLI	0.20	0.11	0.07	0.18	0.08	0.28	0.05	0.12	0.09	0.08	0.37	0.07	0.37	0.27	0.02	0.08	0.25	0.20	0.24	0.05	0.23	0.16
SBLCL	0.43	0.19	0.62	0.32	0.59	0.23	0.59	0.39	0.56	0.33	0.17	0.31	0.25	0.11	0.65	0.62	0.18	0.41	0.49	0.67	0.27	0.40
MLLCL	0.21	0.00	0.28	0.24	0.52	0.26	0.17	0.12	0.36	0.01	0.18	0.00	0.25	0.10	0.61	0.55	0.08	0.11	0.28	0.62	0.02	0.24
03SRH	0.62	0.55	0.24	0.72	0.56	0.48	0.38	0.73	0.42	0.74	0.58	0.75	0.64	0.39	0.32	0.35	0.35	0.78	0.40	0.33	0.68	0.52
01SRH	0.52	0.57	0.09	0.62	0.50	0.23	0.16	0.58	0.27	0.73	0.39	0.70	0.55	0.36	0.13	0.31	0.33	0.72	0.22	0.31	0.55	0.42
7/5LR	0.83	0.64	0.78	0.72	0.85	0.82	0.76	0.76	0.78	0.72	0.74	0.74	0.80	0.88	0.81	0.78	0.84	0.76	0.80	0.78	0.62	0.77
SCP	0.48	0.43	0.26	0.31	0.53	0.37	0.23	0.47	0.31	0.46	0.58	0.46	0.48	0.33	0.13	0.38	0.34	0.46	0.52	0.38	0.32	0.39
STP	0.16	0.00	0.00	0.16	0.00	0.06	0.00	0.03	0.00	0.00	0.20	0.01	0.24	0.30	0.00	0.01	0.25	0.11	0.05	0.00	0.08	0.08
01EHI	0.44	0.12	0.20	0.28	0.43	0.23	0.06	0.36	0.24	0.33	0.36	0.23	0.42	0.29	0.03	0.29	0.22	0.36	0.23	0.28	0.41	0.28
FRZGLVL	0.96	0.87	0.97	0.94	0.95	0.96	0.92	0.93	0.96	0.91	0.96	0.90	0.95	0.93	0.95	0.93	0.90	0.93	0.97	0.94	0.92	0.94
SFC <sub>T<sub>d</sub></sub>	0.49	0.42	0.46	0.49	0.49	0.47	0.41	0.46	0.58	0.42	0.63	0.42	0.60	0.48	0.38	0.49	0.46	0.51	0.49	0.56	0.49	0.49
850 <sub>T<sub>d</sub></sub>	0.12	0.00	0.05	0.40	0.12	0.12	0.00	0.04	0.05	0.10	0.29	0.12	0.10	0.07	N/A	0.02	0.00	0.33	0.11	0.00	0.44	0.12
850WIND	0.88	0.76	0.62	0.83	0.87	0.77	0.66	0.83	0.80	0.87	0.84	0.85	0.86	0.82	N/A	0.88	0.77	0.88	0.84	0.75	0.82	0.81
500WIND	0.93	0.88	0.84	0.90	0.92	0.88	0.85	0.90	0.85	0.88	0.87	0.94	0.92	0.95	0.74	0.85	0.92	0.93	0.86	0.89	0.90	0.89
200WIND	0.93	0.90	0.90	0.92	0.93	0.92	0.89	0.92	0.91	0.94	0.91	0.92	0.93	0.95	0.89	0.93	0.96	0.93	0.90	0.91	0.93	0.92
T <sub>c</sub>	0.71	0.03	0.82	0.78	0.53	0.69	0.21	0.61	0.74	0.07	0.72	0.11	0.70	0.56	0.64	0.76	0.54	0.66	0.74	0.53	0.62	0.56
6BWD	0.88	0.72	0.71	0.86	0.86	0.80	0.78	0.84	0.78	0.81	0.77	0.87	0.86	0.92	0.61	0.77	0.90	0.89	0.74	0.80	0.77	0.81
CB	0.94	0.56	0.91	0.89	0.94	0.92	0.85	0.87	0.92	0.74	0.90	0.82	0.92	0.90	0.91	0.90	0.87	0.89	0.92	0.90	0.84	0.87

TABLE 3. Subjective characterization of parameter  $R^2$  values.

Good	Fair	Poor
7/5LR	SBCAPE	MLCAPE
FRZGLVL	SBLI	SBCIN
850WND	SBLCL	MLCIN
500WND	03SRH	MLLI
200WND	01SRH	MLLCL
6BWD	SCP	STP
CB	01EHI	850 $T_d$
	SFCT $_d$	
	$T_c$	

small errors in the low-level moisture fields may yield large differences in derived quantities such as CAPE. These differences in low-level moisture proved to have an important impact on parcel choice, because all SB

parcel parameters exhibited fair correlation, whereas all ML parcel parameters correlated poorly. To visualize this error, consider the differences in the NARR and observed skew  $T$ - $\log p$  diagrams from Jackson, Mississippi (KJAN), valid 0000 UTC 20 April 2011, when an outbreak of severe thunderstorms was observed across portions of the Ohio and Tennessee Valleys (Fig. 3). Whereas SBCAPE calculations were very similar for NARR and observed soundings (3254 and 3035  $J kg^{-1}$ , respectively; Figs. 4a,c), MLCAPE calculations differed by over 1800  $J kg^{-1}$  (Figs. 4b,d).

Such differences in NARR versus observed low-level moisture fields also influence other variables. In fact, all sites increased correlation values (by an average of 0.17) when examining SB versus ML LCL (Fig. 5). An examination of all 2D histograms suggests that NARR

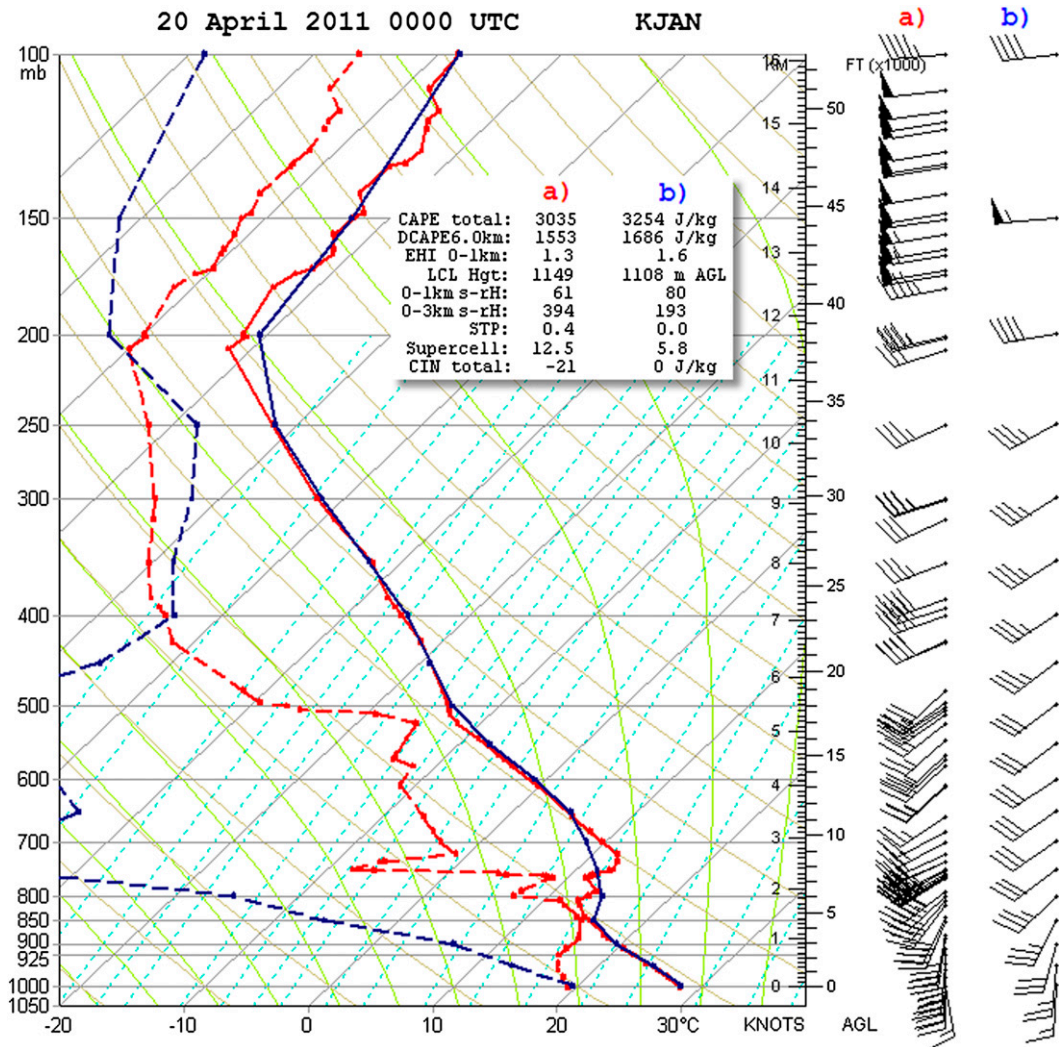


FIG. 3. KJAN observed (red, labeled with “a”) and NARR (blue, labeled with “b”) soundings valid 0000 UTC 20 Apr 2011. Parameters shown are calculated using a surface-based parcel.

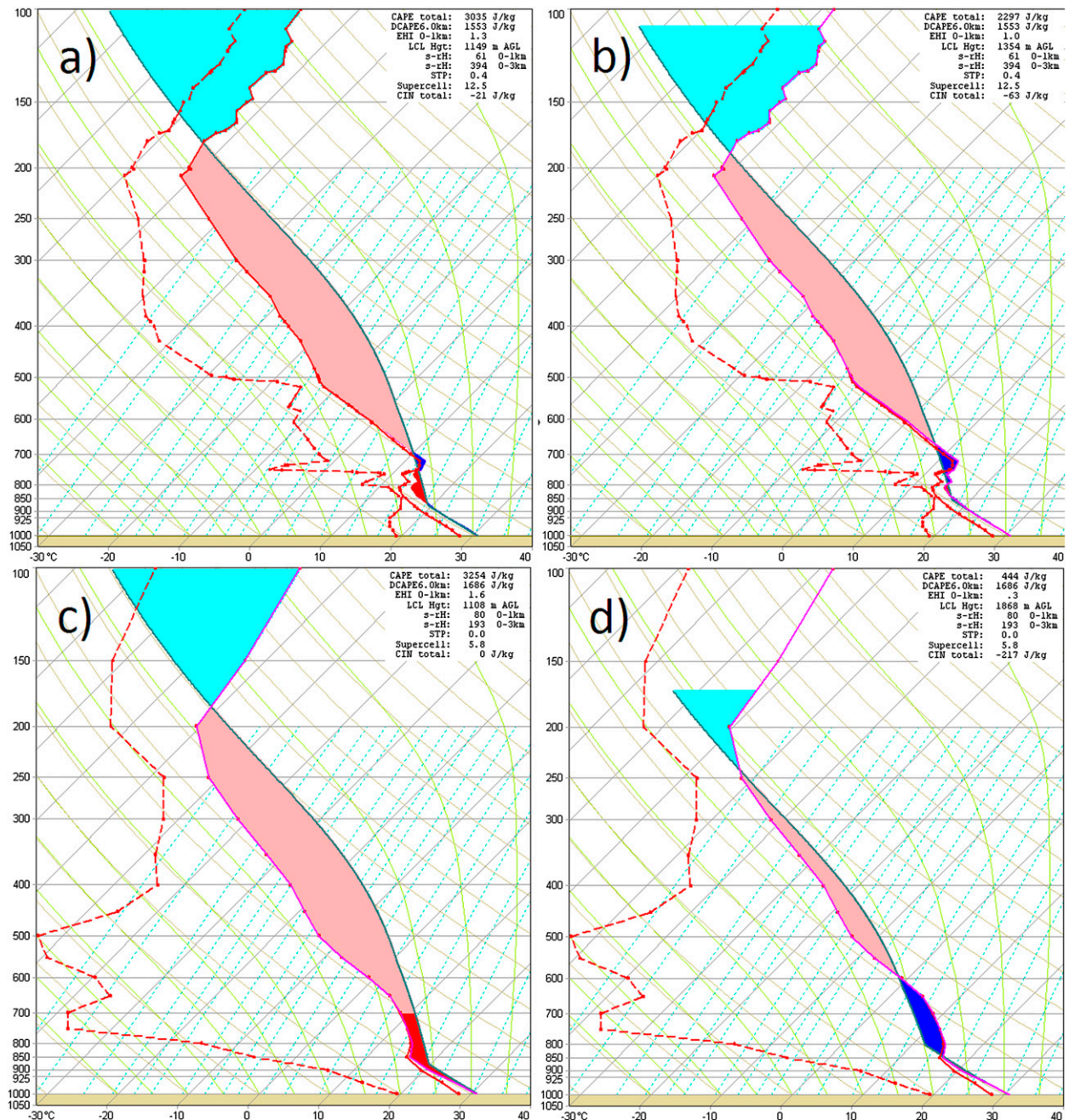


FIG. 4. The 0000 UTC 20 Apr 2011 KJAN (a) SB parcel observed, (b) ML parcel observed, (c) SB NARR parcel, and (d) ML NARR parcel.

variance of MLLCL is too small (Fig. 5b). This error is due to correlation observed with  $850T_d$ .  $SFCT_d$  values exhibited fair correlation, but  $850T_d$  correlation was an average of 0.36 points lower. Thus, an SB parcel using  $SFCT_d$  has a higher probability of lifting a parcel with similar surface moisture values. Averaging the moisture content of the lowest 100 hPa is more likely to inadequately represent the observed convective environment

(especially at higher-elevation locations), however. As a consequence, the improvements to correlation for ML over SB versions of LCL, CAPE, and LI are linked to poor representation of lower-tropospheric moisture, especially in the 925–850-hPa levels. The only exception to parcel choice was CIN, where both SB and ML CIN exhibited poor  $R^2$  values (0.12 and 0.11, respectively).

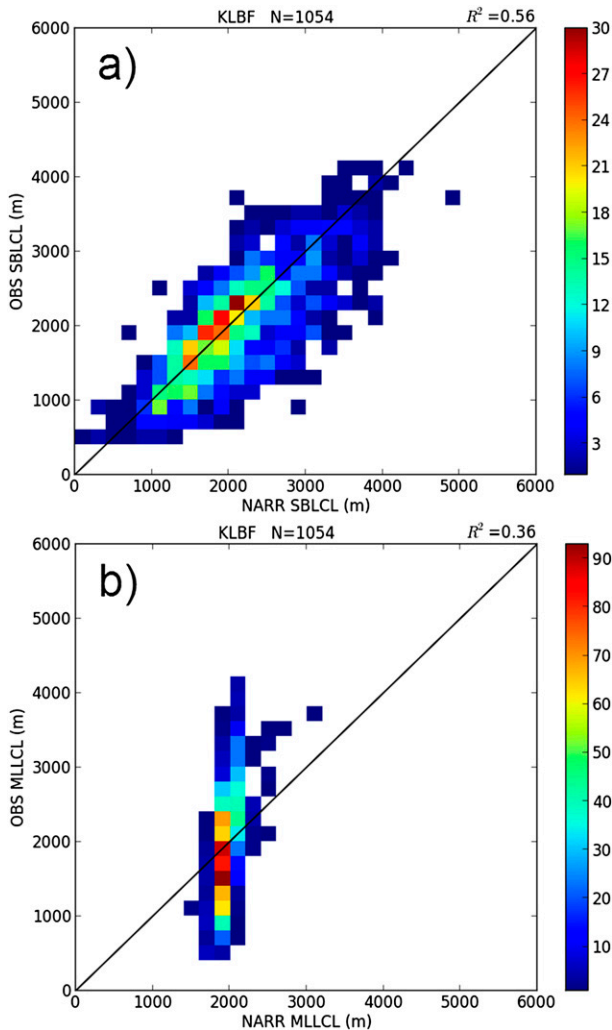


FIG. 5. Comparison of NARR and observed (a) SBLCL and (b) MLCL for North Platte, NE (KLBF), for all events during 2000–11 with nonzero SBCAPE.

### b. Bias/error

Intercept and slope values were calculated for all parameter and station combination linear regression lines (not shown). These values indicate the bias of each group distribution, because they quantify the difference between the parameter subset regression and the 1:1 line (which has an intercept of 0 and a slope of 1). Similar to correlation results, it was found that kinematic parameter values agreed better with observations than did thermodynamic parameters. Nearly all kinematic variables exhibited a linear regression slope of 1 and a  $y$  intercept near 0. In addition, parameters related to midlevel environmental conditions performed better than those calculated from near-surface data. Nearly all bias and error can be traced back to errors in the NARR lower-tropospheric

moisture fields. For instance, the average RMSE for  $850T_d$  at all stations was  $9^\circ\text{C}$  (Table 4). These low-level moisture errors create large RMSE values for variables that depend on the near-surface environment (e.g., SB and MLCAPE station-averaged RMSE values of 1465 and  $1378\text{J kg}^{-1}$ , respectively). Such errors are then compounded in composite parameters such as SCP and STP that utilize CAPE as a measure of static stability.

Large bias and error were also found in CIN fields. In particular, NARR fields commonly underestimated the strength of a temperature inversion associated with the EML. Bias is demonstrated by  $T_c$  slope values near 1, with an average  $y$  intercept near  $4^\circ\text{C}$ , thus indicating that NARR typically underestimates  $T_c$  by roughly  $4^\circ\text{C}$ . Subjective examination of several comparison soundings suggests that rapid vertical changes in temperature associated with the EML are poorly represented in most NARR soundings. This supports the hypothesis herein that NARR inadequately represents sharp temperature changes associated with the EML and results conveyed in previous research (i.e., Brooks et al. 2003; Gensini and Ashley 2011; Allen and Karoly 2014). This bias may be explained by the parameterizations used by the NARR model assimilation. The NARR employs the Betts–Miller–Janjić convective parameterization (Janjić 1990, 1994). Given that errors in  $SFCT_d$  could be considered as acceptable, this suggests that the modeled mixing within the boundary layer is not adequately replicating the convective transport of near-surface moisture throughout the lower troposphere.

## 5. Summary and conclusions

Over 100 000 reanalysis and observed soundings were compared across 21 U.S. upper-air sites during the period 2000–11. This analysis was conducted, in part, to examine how well the reanalysis environment depicts observed and derived variables, specifically focusing on variables related to severe-storm forecasting. In general, kinematic variables are best represented by NARR and thermodynamic variables suffer from errors originating in low-level moisture fields. Therefore, when analyzing NARR convective fields, parcel-ascent choice is an important consideration. Surface-based parcels performed better than 100-hPa mixed-layer parcels, as indicated by less RMSE being found in  $SFCT_d$  fields. Variables best resolved by NARR include 7/5LR, FRZGL, 850WND, 500WND, 200WND, 6BWD, and CB. Large RMSE and low correlation values were found with MLCAPE, SBCIN, MLCIN, MLLI, MLLCL, STP, and  $850T_d$ . Thus, research utilizing NARR low-level fields, and any conclusions drawn from them, should be done with caution.

Overall, NARR provides an invaluable tool to convective researchers because soundings can be derived at



TABLE 4. As in Table 2, but for RMSE values.

	KALB	KAMA	KBIS	KBNA	KBRO	KDDC	KDNR	KDRT	KDVN	KFFC	KGRB	KJAN	KLBF	KLZK	KMAF	KOAX	KOUN	KPIT	KRAP	KTBW	KTOP	Avg
SBCAPE	1215	952	1059	2013	1450	1088	450	1266	2090	1690	1628	2017	1119	2128	945	1619	1254	1915	1218	1809	1653	1456
MILCAPE	889	980	1202	1171	1527	1476	810	1234	2228	1396	1568	1411	1455	1273	950	1798	1380	1677	991	1435	1953	1372
SBCIN	6	8	10	3	5	8	73	6	5	5	4	5	8	6	9	8	8	5	10	6	7	10
MLCIN	60	64	100	20	88	78	125	91	115	89	105	85	75	104	106	114	77	79	87	88	106	88
SBLI	3	2	2	4	2	2	2	4	4	3	4	3	3	4	2	3	2	4	3	3	3	3
MLLI	3	6	3	3	3	3	2	2	4	8	3	9	4	3	10	4	5	4	4	12	4	5
SBLCL	599	632	418	1008	718	357	708	678	538	767	399	939	438	616	545	592	676	495	613	832	463	621
MLLCL	414	1147	576	392	305	578	2494	562	481	1196	469	1331	639	498	2271	512	727	514	891	1723	557	870
03SRH	48	84	90	42	59	105	77	50	66	44	62	46	84	54	59	81	76	49	92	45	73	66
01SRH	43	45	58	34	39	53	41	32	57	44	45	35	64	52	45	56	57	45	54	40	60	48
7/5LR	0	1	0	1	1	0	0	1	0	1	0	1	0	1	0	0	0	0	0	1	0	0
SCP	3	7	4	5	4	6	4	3	6	3	2	5	6	5	3	9	7	3	6	2	6	5
STP	1	0	1	1	1	1	0	1	1	1	1	1	1	1	0	1	1	1	0	1	1	1
01EHI	0	0	1	1	1	1	0	1	1	0	1	0	1	1	0	1	1	1	0	0	1	1
FRZGLVL	165	160	105	237	171	89	448	166	148	219	90	234	101	167	154	116	153	113	107	240	86	166
SFC <sub>T<sub>d</sub></sub>	2	4	3	5	3	2	3	3	3	3	2	4	3	3	3	3	3	2	4	3	2	3
850W <sub>T<sub>d</sub></sub>	7	11	5	4	14	4	N/A	12	5	21	3	20	5	8	16	6	11	2	6	10	15	9
850W <sub>ND</sub>	4	4	4	3	4	4	N/A	3	4	3	4	3	4	4	4	5	4	4	5	4	4	4
500W <sub>ND</sub>	5	4	4	4	4	5	5	4	4	4	5	5	5	5	5	5	4	4	5	4	4	4
200W <sub>ND</sub>	7	7	6	6	6	6	7	6	6	7	7	6	6	7	8	6	6	7	7	8	6	7
T <sub>c</sub>	3	5	3	2	4	4	3	5	4	3	8	3	10	3	9	3	5	2	4	10	3	5
6BW <sub>D</sub>	4	4	4	3	2	3	6	2	3	3	3	3	3	3	4	3	3	3	4	3	3	3
CB	1834	1169	1101	1345	1411	1334	1145	1389	1129	1866	1367	2433	1131	1397	1429	1128	1089	1367	1143	4797	1092	1528

spatiotemporal resolutions much greater than the current radiosonde network. This feature is especially useful for climatological studies that wish to better understand the distribution of environments favorable for severe storms. With these results, bias correction can now be utilized on large-scale climatological studies using similar parameters. Researchers wishing to use NARR fields to initialize model simulations should be aware of potential errors in lower-tropospheric moisture values and sharp vertical changes in temperature associated with an EML. When possible, such initializations should try to correct such errors or supplement NARR fields with observed soundings. Last, researchers using reanalysis datasets to analyze convectively pertinent variables should consider examining their respective parameter biases before application.

*Acknowledgments.* The authors thank Larry Oolman (University of Wyoming) for providing radiosonde data during early stages of this research. In addition, the anonymous reviewers provided valuable feedback on the results of this work.

#### REFERENCES

- Allen, J. T., and D. J. Karoly, 2014: A climatology of Australian severe thunderstorm environments 1979–2011: Inter-annual variability and ENSO influence. *Int. J. Climatol.*, **34**, 81–97.
- Brooks, H. E., J. W. Lee, and J. P. Craven, 2003: The spatial distribution of severe thunderstorm and tornado environments from global reanalysis data. *Atmos. Res.*, **67–68**, 73–94.
- , A. R. Anderson, K. Riemann, I. Ebberts, and H. Flachs, 2007: Climatological aspects of convective parameters from the NCAR/NCEP reanalysis. *Atmos. Res.*, **83**, 294–305.
- Craven, J. P., H. E. Brooks, and J. A. Hart, 2004: Baseline climatology of sounding derived parameters associated with deep, moist convection. *Natl. Wea. Dig.*, **28**, 13–24.
- Doswell, C. A., III, and E. N. Rasmussen, 1994: The effect of neglecting the virtual temperature correction on CAPE calculations. *Wea. Forecasting*, **9**, 619–623.
- Gensini, V. A., and W. S. Ashley, 2011: Climatology of potentially severe convective environments from the North American Regional Reanalysis. *Electron. J. Severe Storms Meteor.*, **6**. [Available online at <http://www.ejssm.org/ojs/index.php/ejssm/article/view/85/68>.]
- Hunter, J. D., 2007: Matplotlib: A 2D graphics environment. *Comput. Sci. Eng.*, **9** (3), 90–95.
- Janjić, Z. I., 1990: The step-mountain coordinate: Physical package. *Mon. Wea. Rev.*, **118**, 1429–1443.
- , 1994: The step-mountain eta coordinate model: Further developments of the convection, viscous sublayer, and turbulence closure schemes. *Mon. Wea. Rev.*, **122**, 927–945.
- Kalnay, E., and Coauthors, 1996: The NCEP/NCAR 40-Year Reanalysis Project. *Bull. Amer. Meteor. Soc.*, **77**, 437–471.
- Lanicci, J. M., and T. T. Warner, 1991: A synoptic climatology of the elevated mixed-layer inversion over the southern Great Plains in spring. Part I: Structure, dynamics, and seasonal evolution. *Wea. Forecasting*, **6**, 198–213.
- Lee, J. W., 2002: Tornado proximity soundings from the NCEP/NCAR reanalysis data. M.S. thesis, Dept. of Meteorology, University of Oklahoma, 61 pp.
- Mesinger, F., and Coauthors, 2006: North American Regional Reanalysis. *Bull. Amer. Meteor. Soc.*, **87**, 343–360.
- Wilks, D. S., 1995: *Statistical Methods in the Atmospheric Sciences*. Academic Press, 467 pp.